Electronic Supplementary Material (ESI) for Soft Matter.

Supplementary information

Bioinspired, electroactive colorable and additive manufactured photonic artificial muscle

Wentao Ma[1], Bo Li[1], Lei Jiang, Ya Sun, Yehui Wu, Pengfei Zhao, Guimin Chen**

Additive Manufacture of FlexAM

Deformation of FlexAM by voltage actuation

Color change of FlexAM under applied voltage

Structural parameters optimization of FlexAM

Fig. S1 to S9

Table S1 to S2

Movie 1. Coloration behavior of Anna's hummingbird's crown and gorget feathers (Courtesy of Mick Thompson for authorization).

Movie 2. Voltage-induced deformation of FlexAM measured by the point laser displacement sensor and the line laser displacement sensor.

Movie 3. Color change response of FlexAM under applied voltages.

Movie 4. Ultrafast color switching of FlexAM under step voltage signal.

Movie 5. Patterns of the photonic display.

Additive Manufacture of FlexAM

The detailed preparation process of photonic layer is shown in Fig. S1a. A silicon wafer, with hexagonal pillar array in nanoscale (period 600 nm, diameter 300 nm, depth 500 nm, and area 20×20 mm^2) on the surface, was used as the template to demold the flexible photonic layer. After 5 minutes of complete mixing with a stirrer and sufficient vacuum degassing, the liquid Polydimethylsiloxane (Sylgard 184) was poured on the silicon wafer template. A film applicator with a preset height is used to cast the liquid Sylgard 184 to ensure its thickness agrees the preset value. After degassing again, the film was cured at 70 ℃ for 3 hours in the oven. Finally, the cured silicone rubber film was carefully peel off from the template to obtain photonic layer.

The multilayer structure of FlexAM includes protective layers, DE layers and compliant electrodes. The protective layer, which plays the role of encapsulating the compliant electrode, was made of a platinum-catalyzed silicone rubber (Ecoflex-0020). The DE layer was prepared of Polydimethylsiloxane (Sylgard 186). A tape casting machine (PF400-H, Lebo, China) was used to fabricate FlexAM, specific preparation parameters include: 100~400 μm for the preset height of the applicator, 5 $mm \cdot s^{-1}$ for the casting speed, 2 mm for the width of the applicator's blade. The casting liquid oligomer is heated at 70 ℃ for two hours to finally obtain a solid film whose thickness is empirically half of the preset thickness. The specific preparation process is shown in Fig. S1b, to help understand, the thickness of DEA is appropriately exaggerated during the process of tape casting multi-layers, (i) Casting the oligomer (Ecoflex-0020) as a protective layer on the substrate by the applicator. (ii) Curing the liquid layer at 70 ℃ for two hours. (iii) The laser-cut PET mask was covered on the dry layer. (iv) Evenly spray the graphite powder on the exposed area of the silicone layer as compliant electrodes by a spray gun. (v) Gently remove the mask. (vi) Casting PDMS oligomer (Sylgard 186, Dow Corning, USA) as the DE film. Repeat step (ii) to (vi) for several times until the number of layers reaches our design. (vii) Casting the final protective layer to encapsulate the electrode. Multilayer structures are obtained by laser-cutting for step (viii). (ix) Attaching the photonic layer on the surface of the DEA. Finally, FlexAM samples were obtained. Because FlexAM and photonic layer are the same material system and have a small amount of viscosity on the surface, they are self-bonded at the surface with a reliable mechanical connection between the two.

Deformation of FlexAM by voltage actuation

Since the nanoscale structure on the surface of the photonic layer will not affect the voltage-induced deformation of the FlexAM, the photonic layer is modelled as a passive layer serving as a mechanical constraint. We give the following assumptions: (i) all deformation is in static equilibrium, (ii) the FlexAM is regarded as an Euler-Bernoulli beam, (iii) the bending deformation of FlexAM along the width direction is negligible, (iv) no slip on the bonding surfaces of the layers, (iv) the thickness of the electrodes is ignored, (v) all silicone layers are considered linear elastic under small deformations. The geometry of FlexAM subjected to an electric field is sketched in Fig. S5 which illustrates the section along the length of a n-layer FlexAM. For any i-th layer, it has a specific Young's modulus Y_i, relative permittivity ε_{ri} and Poisson's ratio v_i. The fixed support point of the bottom surface is defined as the origin of coordinates, the X axis is along the length of the FlexAM and the Z axis is in the thickness direction. The Z-axis coordinates of the upper and lower surfaces of the i-th layer are Z_{i+1} and Z_i, respectively. The radius of curvature of any cross section is ρ. The strain of i-th layer along the X axis can be expressed as:

$$\varepsilon_i = \varepsilon_{i\,Elastic} + \varepsilon_{i\,Maxwell} \tag{1}$$

where the $\varepsilon_{i\,Elastic}$ is the elastic strain by elastic stretch or compress, $\varepsilon_{i\,Maxwell}$ is the strain due to the Poisson effect caused by the Maxwell stress generated by the electric field E in the thickness direction:

$$\varepsilon_{i\,Maxwell} = v_i \frac{\varepsilon_0 \varepsilon_{ri}}{Y_i} E^2 = v_i \frac{\varepsilon_0 \varepsilon_{ri} U^2}{Y_i \left(Z_{i+1} - Z_i\right)^2} \tag{2}$$

Here the ε_0 is the permittivity constant in vacuum (8.852×10^{-12} $F\cdot m^{-1}$), U is the applied voltage. The elastic strain in Equation 1 can be rewritten as: $\varepsilon_{i\,Elastic} = \sigma_i / Y_i$. Assuming the Z-axis coordinate of neutral layer is Z_{na}, for any point on the beam with the coordinate is Z, the axial strain can be written as:

$$\varepsilon_i = \frac{Z_{na} - Z}{\rho} \tag{3}$$

Combining the above equations, the axial stress of any position can be expressed as:

$$\sigma_i = Y_i \left(\frac{Z_{na} - Z}{\rho} - \frac{\nu_i \varepsilon_0 \varepsilon_{ri}}{Y_i \left(Z_{i+1} - Z_i \right)^2} U^2 \right) \tag{4}$$

For the protective layer and photonic layer which no electric field is applied, the relative permittivity is set to zero. For any section perpendicular to the axial direction, the force balance and moment balance can be obtained as:

$$\begin{aligned} \sum F &= \sum_{i=1}^{n} b \int_{z_i}^{z_{i+1}} \sigma_i dz = \sum_{i=1}^{n} b \int_{z_i}^{z_{i+1}} Y_i \left(\frac{Z_{na} - Z}{\rho} - \frac{\nu_i \varepsilon_0 \varepsilon_{ri}}{Y_i \left(Z_{i+1} - Z_i \right)^2} U^2 \right) dz = 0 \\ \sum M &= \sum_{i=1}^{n} b \int_{z_i}^{z_{i+1}} \sigma_i z dz = \sum_{i=1}^{n} b \int_{z_i}^{z_{i+1}} Y_i \left(\frac{Z_{na} - Z}{\rho} - \frac{\nu_i \varepsilon_0 \varepsilon_{ri}}{Y_i \left(Z_{i+1} - Z_i \right)^2} U^2 \right) z dz = 0 \end{aligned} \tag{5}$$

After the derivation, we can obtain the radius of curvature of any point on the neutral layer:

$$\rho = \frac{\frac{1}{4} \left[\sum_{i=1}^{n} Y_i \left(Z_{i+1}^{2} - Z_i^{2} \right) \right]^2 - \frac{1}{3} \sum_{i=1}^{n} Y_i \left(Z_{i+1} - Z_i \right) \sum_{i=1}^{n} Y_i \left(Z_{i+1}^{3} - Z_i^{3} \right)}{\frac{U^2}{2} \cdot \sum_{i=1}^{n} Y_i \left(Z_{i+1} - Z_i \right) \sum_{i=1}^{n} \left(\nu_i \varepsilon_0 \varepsilon_{ri} \frac{Z_{i+1} + Z_i}{Z_{i+1} - Z_i} \right) - \frac{U^2}{2} \sum_{i=1}^{n} \frac{\nu_i \varepsilon_0 \varepsilon_{ri}}{Z_{i+1} - Z_i} \sum_{i=1}^{n} Y_i \left(Z_{i+1}^{2} - Z_i^{2} \right)} \tag{6}$$

In this formula, we find that the radius of curvature is a constant, and it is only related to the material, structural parameters and applied voltage of the FlexAM. Therefore, the deformation of FlexAM is actually a pure bending, and the shape of FlexAM after voltage is a circular arc. The radius of the arc is the radius of curvature obtained in Equation 6. Since the elongation of the FlexAM is sufficiently small that can be ignored with the voltage on, the length of the arc is equal to the length L of the FlexAM before the deformation. We can obtain the deflection angle of the actuator's tip, $\theta_L = L/\rho$. The deflection and the deflection angle are both zero at the fixed end, so the coordinate position of any point on FlexAM neutral layer can be derived as:

$$\begin{cases} x = \rho \sin\theta \\ y = \rho - \rho\cos\theta \end{cases} \quad \theta \in \left[0, \theta_L\right] \tag{7}$$

It should be noted that since the bending deformation of FlexAM is considered as plane strain, the Poisson's ratio and Young's modulus in the above derivation formula need to be corrected as follows:

$$\nu_{i\,plane\_strain} = \frac{\nu_i}{1-\nu_i} \qquad Y_{i\,plane\_strain} = \frac{Y_i}{1-\nu_i^{\,2}} \tag{8}$$

Color change of FlexAM under applied voltage

Based on the fact that we have verified that the angle dependence of photonic layer can be explained by the grating diffraction equation, in this section, we combine the electromechanical response formula derived above and the grating diffraction equation to obtain the coupling between the structural color's wavelength and applied voltage on the FlexAM. As shown in Fig. S6, in the initial coordinate system $X1-Y1$, the parallel light is irradiated on the undeformed FlexAM at the incident angle of θ_i, the observer and the light source are on the same side of the normal, and the observation angle is θ_n. Considering the far distance between the light source and the observer from the FlexAM, the error of the incident angle and the observation angle due to the length of the FlexAM is ignored. After the voltage is applied, the point initially at the position l_0 moves to (x_0, y_0), the deflection angle is:

$$\theta_\alpha = \theta_L \cdot \frac{l_0}{L} \tag{9}$$

The coordinate can be obtained as:

$$\begin{cases} x_0 = \rho \sin\theta_\alpha \\ y_0 = \rho - \rho\cos\theta_\alpha \end{cases} \quad \theta_\alpha \in [0, \theta_L] \tag{10}$$

And the incident angle and observation angle of this point change into $\theta_i - \theta_\alpha$ and $\theta_n - \theta_\alpha$, respectively. According to the grating diffraction equation, the central bandwidth of the structural color that can be observed at this point is:

$$\lambda_i = d\left[\sin\left(\theta_i - \theta_\alpha\right) + \sin\left(\theta_n - \theta_\alpha\right)\right] \tag{11}$$

In order to intuitively obtain the rainbow-like structural color band on FlexAM seen by the observer, the deformed FlexAM is directly projected on a plane perpendicular to the initial observation angle θ_n, which can be expressed as:

$$x_i = x_0 \cos\theta_n + y_0 \sin\theta_n \tag{12}$$

Structural parameters optimization of FlexAM

Based on the results of FlexAM samples with different aspect ratios being used to verify the accuracy of the above theoretical model, we compared the influence of various structural parameters on the electromechanical response in this section. Five main parameters were selected to design the orthogonal experimental calculation and the specific values are shown in Table S1 (The length of the actuator was selected as 15 mm). The calculation results show that the smaller values of the five parameters yield a more significant the bending deformation of FlexAM. However, considering the precision limitations of the fabrication technique and the requirement for FlexAM to have moderate operation output, we have to appropriately compromise on the selection of some of the parameters. By comparing the extreme difference of each parameter (Fig. S7a), we concluded that the thickness of the DE layer and the number of DE layers have the most significant influence on the actuation, and it can be negligible for the rest three parameters. Fig. S7b to S7f indicate the influence of multiple single parameters on the actuation effect on the basis of the optimal parameters obtained by the orthogonal experiment. Finally, we chosen the five parameters P1~P5 as 200 μm, 50 μm, 150 μm, 3 μm and 50 μm. Corresponding tip angle deformation is 29.48° which covers the design goal of 15° proposed in the section of angle dependent characterization of photonic layer.

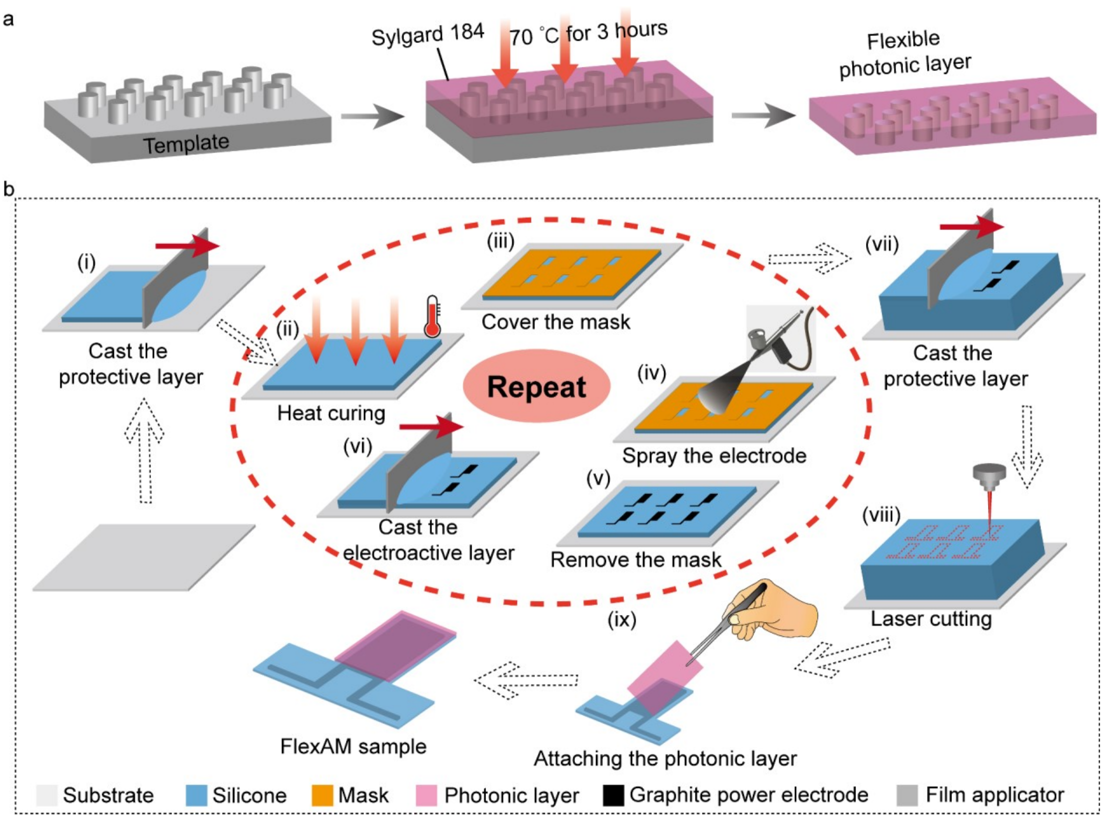

Fig. S1. Fabrication process FlexAM. (a) Fabrication process of photonic layer. (b) Laminate object manufacture (LOM) process of FlexAM.

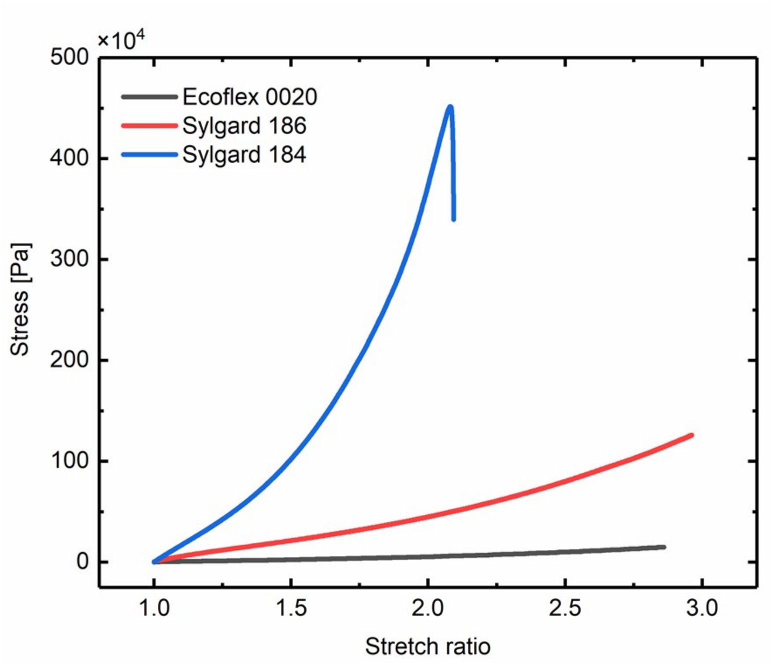

Fig. S2. The relationship between tensile stress and stretch amount of three silicone rubber materials.

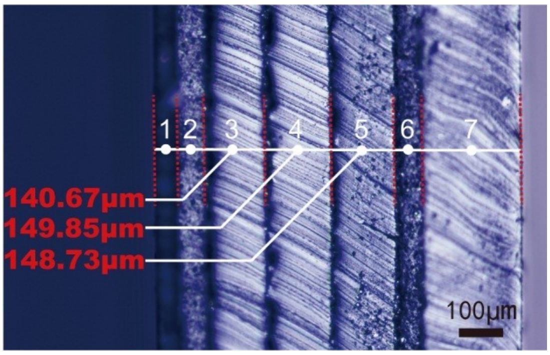

Fig. S3. Cross section of FlexAM under optical microscope, layer 1 is the PET substrate, layer 2 and 6 are the protective layers, layer 3~5 are the DE actuation layers and layer 7 is the photonic layer.

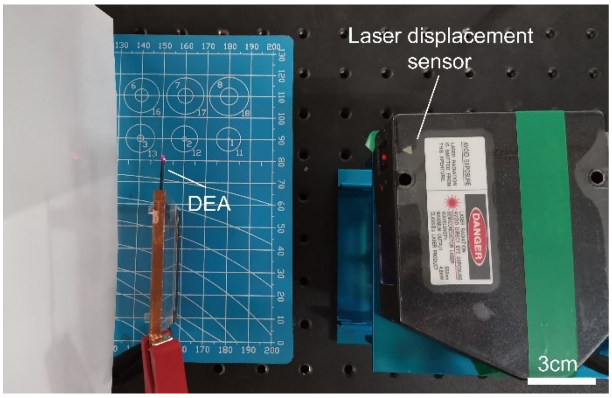

Fig. S4. Experimental setup for measuring FlexAM's tip deflection under cyclic voltage load.

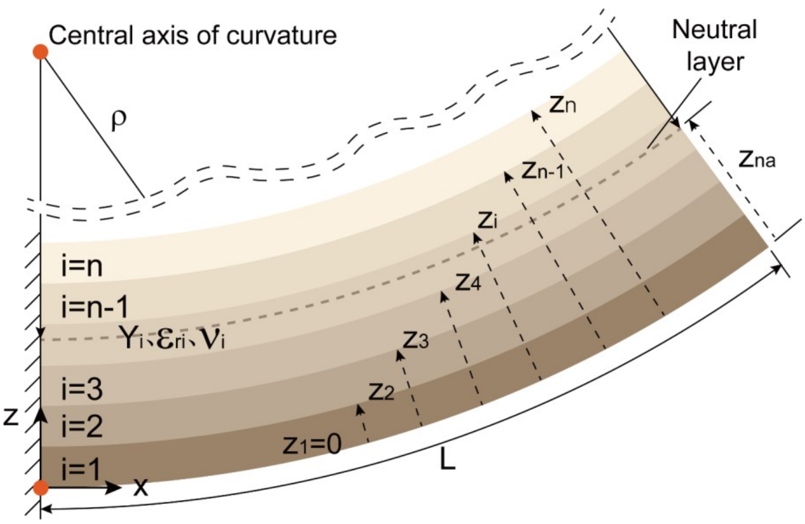

Fig. S5. Geometry of the multi-layer of FlexAM.

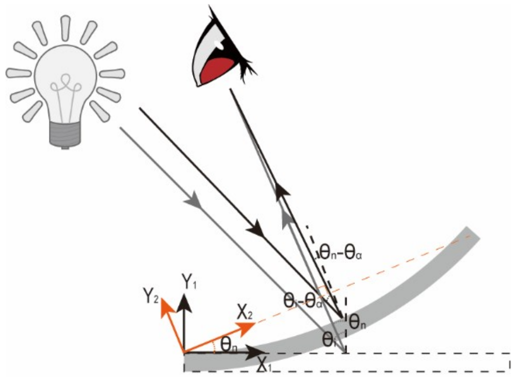

Fig. S6. Diagram of incident angle and observation angle change for FlexAM under applied voltage.

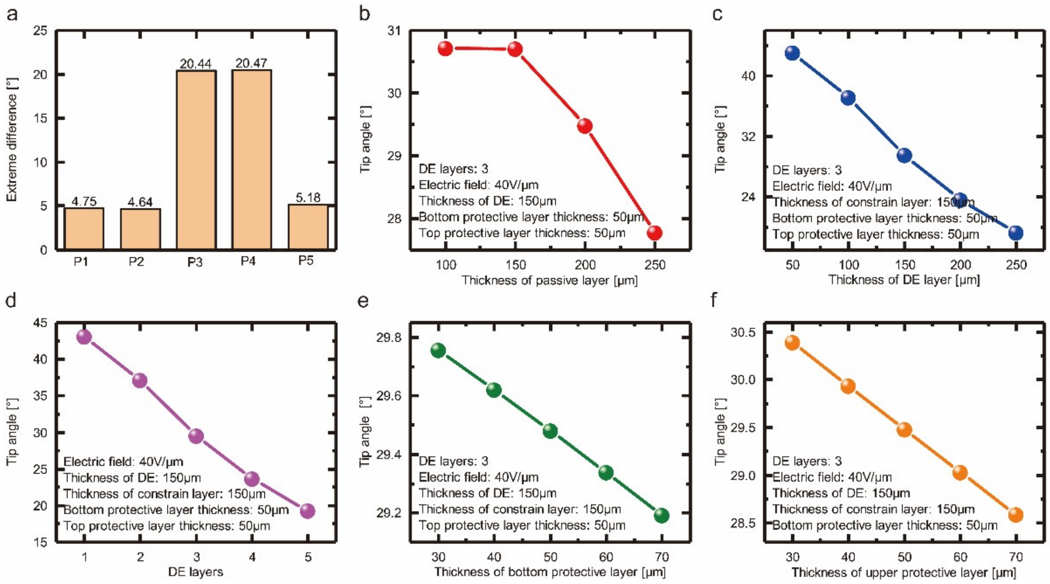

Fig. S7. The influence of each parameter on the actuation effect. (a) The comparison of extreme differences of each parameter derived from the orthogonal experiment calculation. (b)-(d). The influence of multiple single parameters on the actuation performance.

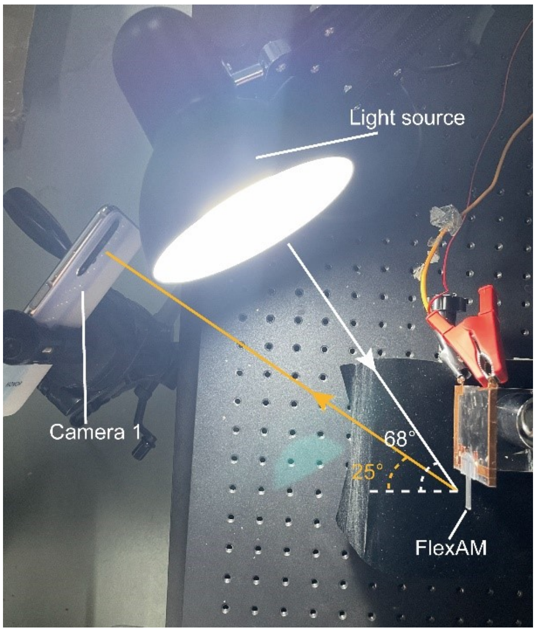

Fig. S8. A camera of the mobile phone is used for recording FlexAM's color change under applied voltage.

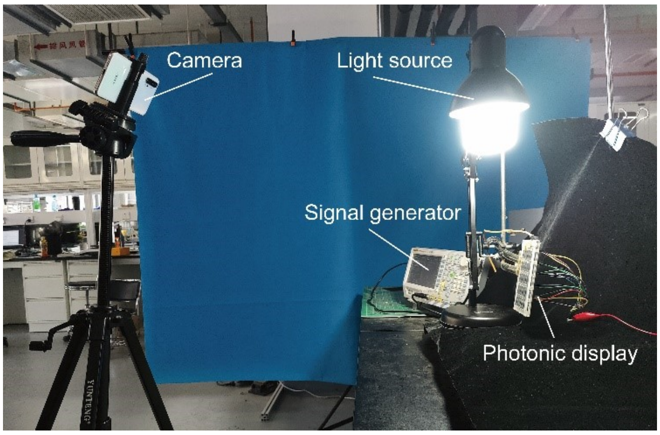

Fig. S9. Arrangement of equipment for recording the patterning process of the photonic display.

Table S1

Parameters and specific values used for orthogonal experimental calculation

Parameters[a)]	Values				Range
Thickness of passive layer [μm]	100	150	200	250	4.75
Thickness of bottom protective layer [μm]	40	50	60	70	4.64
Thickness of DE layer [μm]	100	150	200	250	20.44
DE layer number	2	3	4	5	20.47
Thickness of upper protective layer [μm]	40	50	60	70	5.18

[a)]P1~P5 are used to represent the above five parameters for the convenience of subsequent presentation.

Table S2

The wavelength shift speed and wavelength range in different electrochromic methods

Actuation method	Author	Wavelength [nm]	Range [nm]	Response time [s]	Wavelength shift speed [nm·ms^{-1}]	Reference	Symbols
DE	This work	400-701	301	0.0565	2.814		⊗
DE	Baumberg et al.	673-733 545-569	60 24	0.1	0.6	Ref.[1]	■
DE	Qu et al.	629-737 581-732 600-657	108 151 57	0.5	0.302	Ref.[2]	▲
DE	Sun et al.	485-710	225	2.997	0.075	Ref.[3]	◆
DE	Chen et al.	470-650	180	0.095	0.84	Ref.[4]	★
DE	Ozin et al.	511-613	102	0.87	0.117	Ref.[5]	●
Solvent swelling	Shim et al.	568-633	65	20	0.00325	Ref.[6]	■
Solvent swelling	Puzzo et al.	433-691	258	10	0.0258	Ref.[7]	★
Solvent swelling	Yang et al.	470-620	150	150	0.001	Ref.[8]	●
Solvent swelling	Seo et al.	579.8-626.1	46.3	90	0.0005	Ref.[9]	▲
Solvent swelling	Wang et al.	510-719	209	25	0.00836	Ref.[10]	◆
Solvent swelling	Wu et al.	486-664	178	0.3	0.593	Ref.[11]	⬟
Electrophoresis	Yi	550-700	150	540	0.0003	Ref.[12]	■
Electrophoresis	Lee	480-630	150	0.5	0.3	Ref.[13]	●
Change refractive index	Du et al.	527-630	103	1.7	0.0606	Ref.[14]	■

Change refractive index	Huang et al.	618-661	43	1.5	0.0287	Ref.[15]	
SMA[a)]	Zhao et al.	470-650	180	25	0.0072	Ref.[16]	
TCPF[b)]	Zhao et al.	470-653	183	86.7	0.0021	Ref.[17]	

[a)]SMA represents Shape Memory Alloy; [b)]TCPF represents Twisted and Coiled Polymer Fiber, which is an artificial muscle that shrinks by heat along its length.

References

1. Q. Zhao, A. Haines, D. Snoswell, C. Keplinger, R. Kaltseis, S. Bauer, I. Graz, R. Denk, P. Spahn, G. Hellmann and J. J. Baumberg, *Appl. Phys. Lett.*, 2012, **100**, 4.
2. T. Yin, T. Wu, D. Zhong, J. Liu, X. Liu, Z. Han, H. Yu and S. Qu, *ACS Appl. Mater. Interfaces*, 2018, **10**, 24758-24766.
3. D. Kim, S. Choi, H. Cho and J. Sun, *Adv. Mater.*, 2019, **31**, 6.
4. P. Zhao, Y. Cai, C. Liu, D. Ge, B. Li and H. Chen, *Opt. Mater.*, 2021, **111**, 10.
5. A. C. Arsenault, D. P. Puzzo, I. Manners and G. A. Ozin, *Nat. Photonics*, 2007, **1**, 468-472.
6. T. Shim, S. Kim, J. Sim, J. Lim and S. Yang, *Adv. Mater.*, 2010, **22**, 4494-4498.
7. D. P. Puzzo, A. C. Arsenault, I. Manners and G. A. Ozin, *Angew. Chem.-Int. Edit.*, 2009, **48**, 943-947.
8. Z. Wang, J. Zhang, J. Xie, C. Li, Y. Li, S. Liang, Z. Tian, T. Wang, H. Zhang, H. Li, W. Xu and B. Yang, *Adv. Funct. Mater.*, 2010, **20**, 3784-3790.
9. H. Seo and S. Lee, *Sci Rep*, 2017, **7**, 8.
10. Y. Wang, W. Niu, S. Zhang and B. Ju, *J. Mater. Sci.*, 2020, **55**, 817-827.
11. Y. Lu, C. Meng, H. Xia, G. Zhang and C. Wu, *J. Mater. Chem. C*, 2013, **1**, 6107-6111.
12. H. Lee, S. Kim, H. Lee, K. Park, Y. Kim and G. Yi, *RSC Adv.*, 2016, **6**, 100167-100173.
13. M. Han, C. Heo, H. Shim, C. Shin, S. Lim, J. Kim, Y. Jin and S. Lee, *Adv. Opt. Mater.*, 2014, **2**, 535-541.
14. Y. Wang, H. Cui, Q. Zhao and X. Du, *Matter*, 2019, **1**, 626-638.
15. J. Shi, V. K. S. Hsiao, T. R. Walker and T. Huang, *Sens. Actuator B-Chem.*, 2008, **129**, 391-396.
16. P. Zhao, H. Chen, B. Li, H. Tian, D. Lai and Y. Gao, *Opt. Mater.*, 2019, **94**, 378-386.
17. P. Zhao, B. Xu, Y. Zhang, B. Li and H. Chen, *ACS Appl. Mater. Interfaces*, 2020, **12**, 15716-15725.